Available online at www.sciencedirect.com
SCIENCE DIRECT®
Journal of Hydrology 310 (2005) 294–315
Journal of Hydrology
www.elsevier.com/locate/jhydrol

An infiltration model based on flow variability in macropores: development, sensitivity analysis and applications

Markus Weiler*

Forest Resources Management, University of British Columbia, 2045-2424 Main Mall, Vancouver, BC V6T 1Z4, USA

Received 23 September 2003; revised 31 December 2004; accepted 18 January 2005

Abstract

Simulating infiltration in soils containing macropores still provides unsatisfactory results, as existing models seem not to capture all relevant processes. Recent studies of macropore flow initiation in natural soils containing earthworm channels revealed a distinct flow rate variability in the macropores depending on the initiation process. When macropore flow was initiated at the soil surface, most of the macropores received very little water while a few macropores received a large proportion of the total inflow. In contrast, when macropore flow was initiated from a saturated or nearly saturated soil layer, macropore flow rate variation was much lower. The objective of this study was to develop, evaluate, and test a model, which combines macropore flow variability with several established approaches to model dual permeability soils. We then evaluate the INfiltration–INitiation–INteraction Model (IN^3M) to explore the influence of macropore flow variability on infiltration behavior by performing a sensitivity analysis and applying IN^3M to sprinkling and dye tracer experiments at three field sites with different macropore and soil matrix properties. The sensitivity analysis showed that the flow variability in macropores reduces interaction between the macropores and the surrounding soil matrix and thus increases bypass flow, especially for surface initiation of macropore flow and at higher rainfall intensities. The model application shows reasonable agreement between IN^3M simulations and field data in terms of water balance, water content change, and dye patterns. The influence of macropore flow variability on the hydrological response of the soil was considerable and especially pronounced for soils where initiation occurs at the soil surface. In future, the model could be applied to explore other types of preferential flow and hence to get a generally better understanding of macropore flow.

Keywords: Macropore flow; Infiltration; Soil moisture; Unsaturated zone; Dual-permeability model; Earthworm burrow

1. Introduction

Runoff generation at a site determines the flow pathways in catchments and thus the flow hydrograph for rainfall events. Only a realistic simulation and prediction of flow pathways leads to a correct description of the internal hydrological behavior in a catchment (Beven, 2001). Although the prediction of the flow hydrograph with rainfall-runoff models, which do not account for the relevant runoff processes, may be acceptable, we get 'the right results for the wrong reason' (Klemes, 1986). A correct description

* Tel.: +1 604 822 3169; fax: +1 604 822 9106.
E-mail address: markus.weiler@ubc.ca.

0022-1694/$ - see front matter © 2005 Elsevier B.V. All rights reserved.
doi:10.1016/j.jhydrol.2005.01.010

of the internal hydrological behavior is especially important for the simulation of solute transport processes in the catchment (e.g. nitrate or phosphate leaching) and for the assessment of land-use or climate change scenarios. The influence of macropore flow on hillslope runoff generation is well established (Bronstert, 1999; Faeh et al., 1997; McDonnell, 1990; Návar et al., 1995; Smettem et al., 1991; Weiler et al., 1998; Weiler and McDonnell, 2004), particularly for extreme rainfall events with either a very high intensity for a short duration or a lower intensity for a longer duration. (e.g. Faeh et al., 1997; Niehoff et al., 2002). Despite abundant experimental evidence of its significance, macropore flow, a subtype of preferential flow, is a process that is often not considered in rainfall-runoff models. Indirect evidence of macropore flow at the catchment scale can be obtained through model interpretation (Germann and Beven, 1981; Burch et al., 1989; Niehoff et al., 2002; Beckers and Alila, 2004).

Macropore flow causes a rapid downward movement of water in structural pore spaces such as worm channels, shrinkage cracks, and root holes subsequently bypassing portions of the soil profile. For example, earthworm activity, particularly the anecic earthworm species *Lumbricus terrestris*, causes macropores in soils in humid climate (Langmaack et al., 1999). Macropore flow influences the infiltration of rainfall and therefore the runoff generation and solute transport in natural soils where these structures are common (Larsson, 1999). The impact of macropores is governed to a large extent by water supply to macropores, water flow in macropores, and the water transfer from the macropores into the surrounding soil matrix (Beven and Germann, 1982; Faeh et al., 1997; Buttle and Leigh, 1997). The flow rate in earthworm channels can be very high compared to the rate in the soil matrix. Even for relatively small earthworm channels, the flow rate in macropores seems to be always higher than the rainfall intensity (Bouma et al., 1982; Wang et al., 1994; Shipitalo and Gibbs, 2000; Weiler, 2001). Thus, the flow capacity of the macropore system is usually not the limiting factor during the infiltration process.

Water transfer from macropores into the surrounding soil matrix has been referred to as lateral infiltration from the macropores (Beven and Clarke, 1986). In this study, the term interaction is used to describe this critical process of water flow in structured soils (Logsdon et al., 1996; Faeh et al., 1997). Despite some experiments to measure interaction in single artificial or natural macropores in the laboratory (Smettem, 1986; Ghodrati et al., 1999) or in the field using dye tracers and soil water measurements (van Stiphout et al., 1987), a consistent description, parameterization and verification of the interaction process remains elusive.

Macropore flow initiation is the process of water supply to macropores. It is a function of initial water content, rainfall intensity, rainfall amount, hydraulic conductivity of the soil matrix, and surface contributing area (Trojan and Linden, 1992, Léonard et al., 1999). Water can flow into a macropore if its water entry pressure is exceeded, either at the soil surface or the nearly saturated subsurface (Ela et al., 1992; Li and Ghodrati, 1997; Weiler and Naef, 2003a). Weiler and Naef (2003b) found a distinct distribution of flow rates in macropores depending on where macropore flow is initiated.

The objective of this study was to develop, evaluate and test a model that combines well-known approaches of simulating initiation and interaction with the yet uncommon initiation-based flow rate distribution. This model was then used as a tool to evaluate the hypothesis that the initiation process is crucial to infiltration in macroporous soils and hence to runoff generations in general. This hypothesis was tested theoretically with a sensitivity analysis evaluating for a synthetic dataset the influence of the initiation process on interaction and on the hydrological response of the soil. The new conceptual framework of the model was tested practically by simulating results from sprinkling experiments at three field sites in Switzerland (Weiler and Naef, 2003a).

2. Model theory

The INfiltration-INitiation-INteraction Model (IN^3M) allows for water flow within discrete macropores, as well as for water flow in the soil matrix based on the dual permeability concept. Analytical solutions of the Green-Ampt equation and a simple accounting scheme serve as the basis for the model. The use of analytical solutions removes any concern regarding

the numerical instability observed in most preferential flow codes (Simunek et al., 2003) and results in code that can be more readily incorporated into distributed rainfall-runoff models. In the following, we give a detailed description of the model theory for the processes of initiation and interaction and how they are combined within IN^{3}M. We furthermore suggest a multi-criteria validation that includes the comparison of observed and artificially generated dye patterns.

2.1. Process of macropore flow initiation

Detailed studies of initiation of macropore flow from the soil surface and the subsurface have concluded that only a few macropores contribute significantly to the total macropore flow (Weiler and Naef, 2003b; Léonard et al., 2001). The inflow quantity of each macropore is proportional to its macropore drainage area (MDA), which is defined as the area that drains to a macropore. The inflow $qin(t,i)$ into a macropore i is then given as (Weiler and Naef, 2003b):

$$q_{\text{in}}(t,i) = (I(t) - i_{\text{mat}}(t))\text{MDA}_i\, n_{\text{mac}} \quad (1)$$

with the total input I (precipitation or matrix outflow from upper layer), the infiltration rate into the soil matrix i_{mat}, and the macropore density n_{mac} (L-2). This relation assumes uniform rainfall distribution, a homogeneous hydraulic conductivity of the soil matrix, and a sufficient flow capacity of each macropore.

The distribution of flow rates in macropores for subsurface initiation, which is symmetrical and has a low variance, was found to be distinctively different from the distribution for surface initiation, which is highly skewed and has a high variance (Weiler and Naef, 2003b). This difference of the initiation process has to be considered in the model. Weiler and Naef (2003b) derived distributions of MDA for surface initiation and for subsurface initiation under steady and non-steady state conditions. Their results are shown in Fig. 1, where the MDA of each macropore was normalized by the mean MDA; that is the surface area multiplied by the macropore density.

For subsurface initiation, the dynamic simulation resulted in similar probability distributions as for the steady-state assumption that the distribution of the MDA is equal to the size distribution of random Voronoi segments, if the macropores are randomly distributed in space with an areal density equal to the macropore density (Weiler and Naef, 2003b). This distribution can be derived for 1D: (Kiang, 1966)

$$f(x) = \frac{c}{\Gamma(c)}(cx)^{c-1}\, \mathrm{e}^{-cx} \quad (2)$$

where the Gamma distribution has the shape parameter $c=2$ for the 1D case and x is the standardized length. For the 2D case, the distribution becomes difficult to establish and no rigorously derived result has been published in the literature to date. However, simulations with randomly generated point patterns showed that c was equal to 4 (Kiang, 1966).

Similar to the distribution of the MDA for subsurface initiation, a distribution can also be derived for surface initiation (Fig. 1). A theoretical probability distribution was fitted to the simulation results of the MDA frequency distribution using a non-linear least squares fitting procedure. The Weibull distribution was chosen because it is an extreme value distribution and it can have exponential or symmetrical behavior. The probability distribution function (pdf) takes the form:

$$f(x) = \frac{\beta}{\lambda}\left(\frac{x}{\lambda}\right)^{\beta-1}\exp\left[-\left(\frac{x}{\lambda}\right)^{\beta}\right] \quad (3)$$

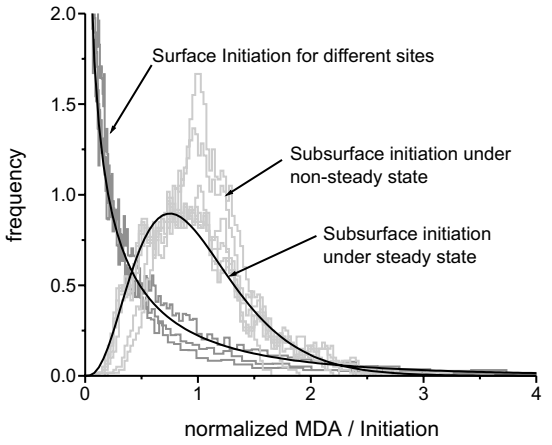

Fig. 1. Frequency distribution of the macropore drainage area for surface and subsurface initiation and simulation results for surface initiation. Modified from Weiler and Naef (2003b) with addition of the average probability density function for surface and subsurface initiation.

with the two parameters β and $\lambda > 0$. Simulations by (Weiler and Naef, 2003b) showed that the derived parameters, and thus the distribution of the MDA, are quite similar for different macropore densities (Fig. 1). Consequently, an average pdf with $\beta = 0.66$ and $\lambda = 0.55$ was optimized and is also plotted in Fig. 1.

2.2. Processes of interaction and water flow in the soil matrix

To explore the effects of variations of water flux in the macropores due to the initiation process, a relative simple dual permeability model was conceptualized that combines well-known approaches to describe the individual controlling processes of infiltration in macroporous soils. In addition to macropore initiation, the water transfer from the macropores into the surrounding soil matrix (interaction) still represents one of the greatest challenges of successfully describing preferential flow (Simunek et al., 2003). The description of interaction can be very complex due to the high number of influencing factors. These factors influencing interaction can be subdivided into properties of the soil matrix, of the macropores, and the macropore–matrix interface. Interaction, which can be described as the horizontal infiltration in an unsaturated soil matrix, is governed by the soil water characteristics, the unsaturated hydraulic conductivity, and the initial moisture conditions of the soil. The macropore system can be described by the macropore density and the geometry of the macropores, which both control the surface area of the interface between the macropores and the soil matrix. This study concentrates on macropores formed by anecic earthworms, and the geometry of the macropores can therefore be simplified as vertically oriented, circular tubes (Syers and Springett, 1983).

Two different approaches have been used to model horizontal infiltration with radial symmetry based on: (1) the saturation deficit of the soil matrix or (2) the potential gradient between the macropores and the soil matrix (see for detailed comparison Simunek et al., 2003). The first approach relies on constant boundary conditions at the macropore wall (Beven and Clarke, 1986; Jarvis et al., 1991; Chen and Wagenet, 1992; Ahuja et al., 2000). The second approach describes interaction as a linear function of the driving potential in analogy to the Darcy equation (Workman and Skaggs, 1990; Faeh et al., 1997) or as a steady state flow from a water filled borehole (Smettem, 1986). Simunek et al. (2003) demonstrated that despite the different approaches to describe interaction, only very small differences were notable comparing water mass exchange and water content profiles in the soil matrix. This suggests that an appropriate description of interaction may depend less on chosen approach than on the parameterization of the approach. Thus, a well-known and relative simple approach introduced in the RZWQM model (Ahuja et al., 2000) was chosen to describe vertical infiltration in IN^{3}M. In order to avoid the use of a numerical-based model, we derived analytical solutions for vertical and horizontal infiltration based on the Green-Ampt assumptions.

For a cylindrical shape of the macropores, a predominant horizontal movement of water from the macropores into the soil matrix, and a complete wetting of the macropore/matrix interface, the Green-Ampt assumptions (Green and Ampt, 1911) for horizontal infiltration with radial symmetry are valid (Beven and Clarke, 1986):

$$\frac{\mathrm{d}y}{\mathrm{d}t} = \frac{K_s r(h + \psi_f)}{y\,\Delta\theta(y - r)} \tag{4}$$

where y is the radial distance of the wetting front from the center of the channel, r is the radius of the macropore, K_s is the saturated hydraulic conductivity of the soil matrix (at the tension that is determined by the size of the macropores, e.g. if $r = 3$ mm that the water entry tension is 0.5 cm), h is the positive pressure head in the macropore (under free-flowing condition in the well-ventilated earthworm channels $h = 0$ cm), $\Delta\theta$ is the change of water content across the wetting front, and ψ_f is the wetting front suction. The Green-Ampt model further assumes that the soil matrix is initially uniformly dry with a water content of θ, that a distinct wetting front during infiltration exists, that the wetting front suctions remain constant in time and space, and that the soil behind the wetting front is uniformly wet with a constant hydraulic conductivity (Beven and Clarke, 1986). For $y = r$ at

time $t=0$ Eq. (4) can be solved for time t:

$$t = \frac{\Delta\theta}{K_s r(h+\psi_f)}\left(\frac{y^3}{3} - \frac{y^2 r}{2} + \frac{r^3}{6}\right) \quad (5)$$

For Eq. (5) a real solution can be found for the radial distance of the wetting front y at a given time t:

$$y(t) = \frac{1}{2}\frac{b^{(1/3)}}{\Delta\theta} + \frac{1}{2}\frac{a}{b^{(1/3)}} + \frac{1}{2}r \quad (6)$$

$$a = \Delta\theta r^2 \quad (6a)$$

$$b = r\,\Delta\theta^2(12c - a + 2\sqrt{6}\sqrt{c(6c-a)}) \quad (6b)$$

$$a = tK_s(h+\psi_f) \quad (6c)$$

Beside the wetting front suction, all parameters can be directly determined from soil properties and initial conditions. The soil water retention curve and unsaturated hydraulic conductivity curve is used to calculate the wetting front suction (Mein and Larson, 1973):

$$\psi_f = \int_{K_{ro}}^{1} h(K_r)\mathrm{d}K_r \quad (7)$$

where $h(K_r)$ is the inverse function of the relative hydraulic conductivity $K_r(h)=K(h)/K_s$and K_{ro} is the relative hydraulic conductivity at the initial soil water content θ of the soil. Thus, the wetting front suction is a function of the initial soil water content, the shape of the water retention curve, and of the unsaturated hydraulic conductivity curve. The wetting front suction will be highest at the residual water content and zero at saturation.

Eq. (6) give the solution of the radial distance of the wetting front y for any time. The interaction q_{int} (horizontal water flux from the macropores into the soil matrix) for any time t can be calculated for a soil layer with a given height Δz and for one vertically oriented macropore with:

$$q_{int}(t) = \pi[y(t)^2 - y(t-\Delta t)^2]\frac{\Delta z\,\Delta\theta}{\Delta t} \quad (8)$$

where Δt is the time step and $y(t)$ is the radial distance of the wetting front at time t and $y(t-\Delta t)$ is the radial distance of the wetting front at the previous time.

The vertical infiltration in the soil matrix is calculated like the horizontal infiltration using the Green-Ampt approach (Green and Ampt, 1911):

$$I = K_s\frac{\psi_f + h_0 + z_{wf}}{z_{wf}} \quad (9)$$

where I is the infiltration rate, h_0 is the depth of the surface ponding, and z_{wf} is the depth of the wetting front. The wetting front suction is calculated with Eq. (7). Since IN^{3}M should be applicable to natural soils that consist of soil layers with different hydraulic properties, an approach to apply the Green-Ampt equation to a multi-layer soil was used (Schiffler, 1992). Between rainfall events soil water redistribution is simulated with the Buckingham-Darcy law of vertical water flow:

$$J_w = K(\theta)\left(1 + \frac{d}{\mathrm{d}z}h\right) \quad (10)$$

where J_w is the volumetric water flux and the potential gradient is estimated using the geometric mean of the matric potential in the layers (Schiffler, 1992). The lower boundary condition can be specified as unit gradient, constant flux or constant pressure head.

2.3. Model structure and parameters

IN^{3}M combines the variable water flow in macropores distributed according to the initiation process with the vertical water flow in the soil matrix and the horizontal water flow from the macropores into the soil matrix (interaction). Therefore, it is necessary to simulate simultaneously water flow and interaction in several macropores. The vertical water flow in the soil matrix is calculated in 1D. Several layers with different soil properties and initial conditions can be considered. Fig. 2 illustrates the structure, variables, and flow of information within one layer.

Macropore flow is initiated at the upper boundary of a layer if the upper inflow into this layer exceeds the infiltration capacity of the soil matrix. The excess water is transferred to the macropore domain and distributed into the simulated macropores according to the distributions for surface (Eq. (3)) or subsurface (Eq. (2)) initiation. Surface initiation occurs only at the upper boundary of the top layer, subsurface initiation at the other boundaries.

A simple but efficient accounting scheme, which moves water to the next layer if it cannot be taken up

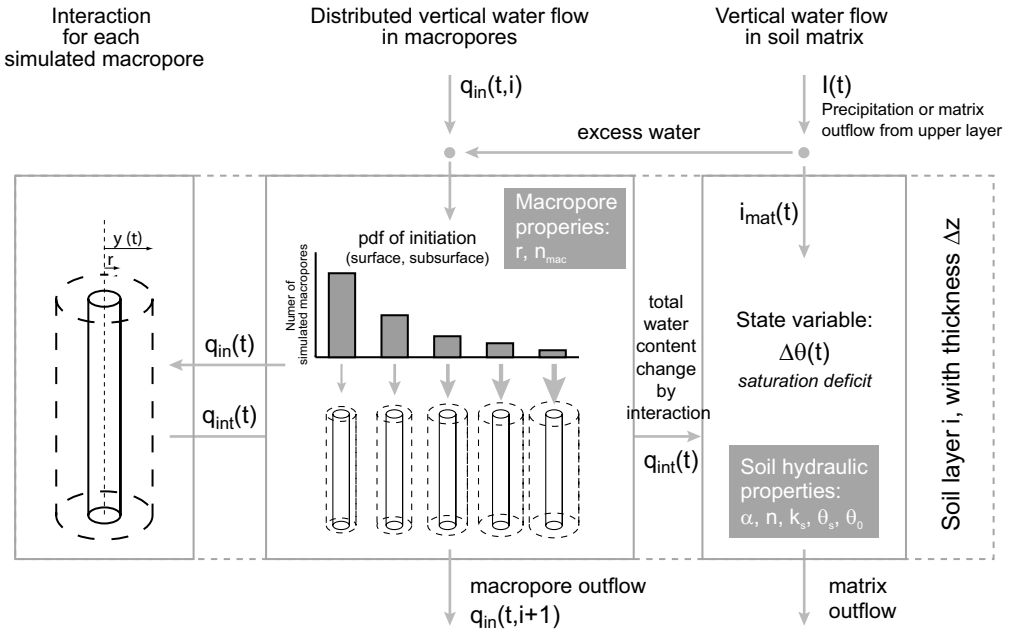

Fig. 2. Structure, variables, and flow of information within one layer of IN^{3}M.

from the previous layer (Ahuja et al., 2000), is then used to calculate water fluxes and water content changes in each layer from top to bottom.

(i) *Vertical matrix infiltration*. the vertical water flow in the soil matrix is calculated by Eqs. (9) and (10). Then excess water, which is the water that cannot infiltrate into the soil matrix of layer i, is added to the macropore outflow from the layer above resulting in the macropore inflow q_{in}.

(ii) *Saturation check.* when the soil matrix of layer i is saturated, interaction $q_{int}=0$, and thus $q_{in}(t, i=1)$ of the next layer is equal to macropore inflow of layer i (the retarding influence on interaction by neighboring macropores is not considered)

(iii) *Start of interaction.* when $q_{in}(t)$ exceeds zero for the first time, interaction begins. The potential radial distance of the wetting front $y_{pot}(t)$ is calculated with Eq. (6). The radial distance of the wetting front that is limited by the inflow into the layer $y_{in}(t)$, is calculated with Eq. (7), which is solved for $y(t)$ with $q_{int}(t)=q_{in}(t)$.

(iv) Comparison of actual y_{in} and potential y_{pot} radial distance of wetting front: If $y_{in}(t)>y_{pot}(t)$, the inflow into the layer is greater than the potential interaction, the actual interaction $q_{int}(t)$ is calculated with Eq. (8) with $y(t)=y_{pot}(t)$. The time for interaction of this layer is set to $t+\Delta t$. The outflow of this layer that is equal to the inflow of layer $i+1$ is calculated with $qin(t,i+1)=qin(t,i)+qint(t,i)$.

If $y_{in}(t)\leq y_{pot}(t)$, the inflow into the layer is smaller than the potential interaction, the actual interaction has to be reduced to the inflow by adjusting the time for calculating the interaction. This time is calculated with Eq. (5) with $y=y_{in}(t)$. The actual interaction $q_{int}(t)$ is equal to the inflow $q_{in}(t,i)$ and the outflow $q_{in}(t,i+1)=0$.

(v) *Water content in the soil matrix* is adjusted by balancing vertical matrix infiltration, matrix outflow and the sum of actual interaction $q_{int}(t)$ of all simulated macropores.

(vi) *Lower boundary condition of the macropore domain* is either defined by the end of a macropore (dead-end macropore) in one layer or by the maximum outflow of the macropores q_{max} if the macropores end at the lower boundary. This parameter can either be set to

zero, if one assumes no direct connection of the macropores with other lateral preferential flow structures (default) or to any number describing the potential flow in lateral preferential flow structures (e.g. based on a distributed hillslope or catchment model). For any case, when the outflow of one layer is smaller than the inflow, the macropores will fill up and the now positive pressure head in the macropore h will increase interaction. If the water table in the macropores reaches the soil surface, overland flow will start.

The input parameters for IN^{3}M describe soil properties and initial and boundary conditions. The soil properties are parameterized by:

(a) the number and thickness Δz of individual layers;
(b) the soil hydraulic properties of each layer which are described by the equation of van Genuchten (1980), where θ_s is the saturated water content, θ_r is the residual water content, α is a scaling parameter that is inversely proportional to the mean pore diameter, n is the pore size distribution index, and K_s the saturated hydraulic conductivity;
(c) the macropore properties of each layer, which are characterized by the macropore density n_{mac} and the average macropore radius r.

The parameters for initial and boundary conditions are: (1) time series of precipitation, (2) the initial average water content θ of each layer, and (3) the maximum outflow of the macropore domain at the lower boundary q_{max}.

2.4. Generation of dye patterns

Preferential flow research in the vadose zone relies heavily on the use of dye tracer experiments and the interpretation of dye patterns (Flury and Wai, 2003). Hence, a tool was developed to generate artificial dye patterns from the simulation results of IN^{3}M. A comparison of experimental dye patterns with dye patterns from simulations is a potentially powerful method to validate dual porosity models and to visualize the simulated preferential water flow. Dyes that have been used in vadose zone hydrology (e.g. Brilliant Blue FCF) show sorption behavior that may even change when the dye travels through different subsurface media (Flury and Wai, 2003). To account for this complex retardation process would require a detailed knowledge about the dye's sorption behavior, which often is not known in hydrological field studies. Given this uncertainty, dispersion, adsorption and retardation could not be accounted for in the dye pattern tool. The following methodology generates the artificial dye patterns:

(1) A soil block is reproduced by a 3D array with a horizontal resolution of 1 mm and a vertical resolution of 10 mm. The horizontal size is arbitrarily set to 800 by 400 mm and the vertical size depends on the total thickness of simulated soil layers.
(2) An artificial macropore network in the soil block is generated using the parameterized macropore density of each soil layer. A point pattern of spatially random distributed macropores at the top border is generated. Then the position of each macropore in the pixel layer below is determined. The horizontal displacement is calculated by two independent normally distributed random numbers X and Y with a mean of zero and a standard deviation of 0.4 times the vertical resolution. The angle of the macropore from the vertical α is also a random number and calculated with:

$$\alpha = \arctan(\sqrt{X^2 + Y^2}) \quad (11)$$

The resulting cumulative probability distribution of the macropore network inclination corresponds well to the measured distribution of nine casted earthworm burrows (Weiler, 2001) with the simulated distribution having a mean of 24.4° and a 20 and 80% percentile of 14.1 and 35.7° and the measured distribution having a mean of 23.4° and a 20 and 80% percentile of 11.5 and 30.9°. The simulated distribution also corresponds with the frequency distributions of inclination of earthworm macropore networks measured with computer tomography (Perret et al., 1999) and from excavating and recording the macropore networks (Ligthart and Peek, 1997).

(3) Starting from the center of the macropores, the staining around the macropores is generated. Staining around the macropores is based on

the probability distribution of the radial distances of the wetting front of each soil layer. This distribution is an output of IN^{3}M, where the radial distance of the wetting front y for each simulated macropore is calculated for each time step. Thus, the probability distribution can be derived for each soil layer. The radial staining distance y_{st} is then calculated by:

$$y_{st} = (y - r)\frac{\Delta\theta}{\eta(\theta_s - \theta_r)} + r \quad (12)$$

where η is the effective fraction of the maximum saturation deficit, in which the transport of the tracer took place. The calculation of the staining distance assumes only advective transport of the tracer. The values of the probability distribution of y_{st} determined the radius of the circle that was used to define the staining around the macropores. The allocation of y_{st} to a macropore is random.

(4) Finally, the depth of the homogeneous staining of the soil matrix from the soil surface is calculated. The depth depends on the input into the soil matrix and the maximum soil moisture deficit. Only advective transport is assumed.

The resulting dye pattern is a 3D array with stained and unstained marked voxels. This 3D array is then sliced into 10 vertical sections from which the average depth function of the dye coverage is calculated for comparison with the field experimental results.

2.5. Model validation

The validation of models has been a topic of discussion in the scientific community for decades (Klemes, 1986). Usually a 'goodness-of-fit' measure is used to determine the degree to which the model simulations match the observations. However, these measures are over-sensitive to extreme values and are insensitive to additive and proportional differences between model predictions and observations (Legates and McCabe, 1999). Furthermore, for direct comparison, observed and simulated results must occur in the same time and space scale. Also, the limitation of the device measuring the observed values should be taken into consideration. In light of these difficulties, validation using multi-response data, also called multi-criteria validation, is the best way to verify the model hypotheses (Seibert and McDonnell, 2002). Such a verification is particular important for new model concepts.

To evaluate IN^{3}M, a multi-criteria validation strategy was developed and applied. The strategy was built on three different criteria that were examined qualitatively in the following ways: (i) a water content change criterion by depth–time plots of water content change, saturation of the soil matrix, and final water content change in the soil matrix, (ii) a dye pattern criterion by visual comparison of observed dye staining patterns with those generated by the model, and (iii) a water balance criterion by comparison of the measured with simulated total fluxes and water content changes.

3. Sensitivity analysis

3.1. Strategy

Since IN^{3}M can simulate the flow rate distribution in macropores, the influence of initiation on interaction and thus on the vertical flow in the macropores and on the water content change in the soil matrix can be analyzed under the model assumptions. For this purpose the simulation of vertical water flow in the soil matrix was switched off and simulations were run for three different conditions of water flow distribution in the macropores at the upper boundary:

(a) same flow rate in each macropore (neglecting the initiation process)
(b) flow rate distribution according to surface initiation (Weiler and Naef, 2003b and Fig. 1)
(c) flow rate distribution according to subsurface initiation (Weiler and Naef, 2003b and Fig. 1).

A typical loamy subsoil was parameterized with a depth of 50 cm. The soil properties were set to $\alpha = 1.4\ m^{-1}$, $n = 1.4$, $\theta_s = 0.41$, $\theta_r = 0.06$, $\theta = 0.21$, $\Delta z = 20$ mm, and $K_s = 10\ mm\ h^{-1}$, which corresponds to a wetting front suction $\psi_f = 126$ mm and a total soil moisture deficit of 100 mm. The chosen macropore properties of $n_{mac} = 100\ m^{-2}$ and $r = 3$ mm were found to be typical for a macropore system built by

the earthworm species *Lumbricus terrestris* (Weiler and Naef, 2003b). The total inflow rate q_{in} into the macropore system was then varied between 5, 10, 20, and 40 mm h^{-1}, while, the total inflow was always 100 mm, which is equal to the total soil moisture deficit of the soil matrix.

3.2. Influence of the initiation process

The influence of initiation on interaction for the three different conditions of water flow distribution in the macropores and different input intensities was analyzed by comparing measures representing the total, spatial, and temporal interaction process. The first measure is the total water content change in the soil matrix which is calculated in place of the total interaction. The second measure is the temporal water content change in the soil matrix. The third measure is the temporal change of total flow in the macropores at the lower boundary.

Generally, the total water content change in the soil matrix decreases with an increasing input rate due to increased bypassing of the soil matrix (Table 1). In addition, the initiation process influences the water content change in the soil matrix. Especially for the flow rate distribution for surface initiation, the total water content change is 15–42% lower than for the simulations with the same flow rate in every macropore (Table 1). But also for the flow rate distribution for subsurface initiation, the total water content change is around 2–11% lower compared to the simulations with the same flow rate (Table 1).

Fig. 3 shows the temporal water content change in the soil matrix as a function of soil depth z for the three different upper boundary conditions. For the lowest input rate (5 mm h^{-1}), the potential interaction is higher than the input. Thus, for the same flow rate in every macropore the wetting front in the soil matrix moves from the top to the bottom similarly to infiltration in a soil without macropores. The shape of the water content profiles for the flow rate distribution of subsurface initiation shows a tailing with depth. This tailing is even more pronounced for surface initiation. The shape of the water content profiles obviously depends on the distribution of flow rates in the macropores. For example, for the surface initiation distribution the higher flow rate in some macropores results in a faster penetration of water in these macropores, as the interaction is lower than the flow rate into the macropores. Therefore, the water content increases almost immediately over the whole soil profile. When the input rate is increased, the average water flow in the macropores becomes large compared to the potential interaction. Thus, the water content profiles are more elongated in the vertical direction. This elongation is even more pronounced for higher input rates. If a soil layer gets saturated, the interaction suddenly falls to zero and the water flow in the macropores increases. The result is a break in the water content profile that can be observed for the simulation of the same flow rate in every macropore with a rate of 5, 10 and 20 mm h^{-1}. This break cannot be seen for the simulation with a flow rate distribution, as the total interaction in a layer is smaller than for the simulation without distribution.

Fig. 4 shows the influence of the initiation process on the total flow in the macropores at the lower boundary for the four different input rates. The outflow is shown as outflow ratio that is the outflow rate divided by the inflow rate. This outflow ratio is plotted as a function of the input for better comparison of the results. The simulated outflow can also be considered as the hydrological response of the soil. For the lowest input rate of 5 mm h^{-1}, the outflow for the three different upper boundary conditions differs considerably. For the simulation with the same flow rate in every macropore, the outflow suddenly increases near the end of the simulation after the wetting front has

Table 1
Total water content change in the soil matrix due to different initiation processes with 100 mm of inflow

Initiation process	Water content change (mm) for different input rates			
	5 mm h^{-1}	10 mm h^{-1}	20 mm h^{-1}	40 mm h^{-1}
Same flow rate in every macropore	98	96	91	83
Flow rate distribution for subsurface initiation	96	92	85	74
Flow rate distribution for surface initiation	83	73	62	48

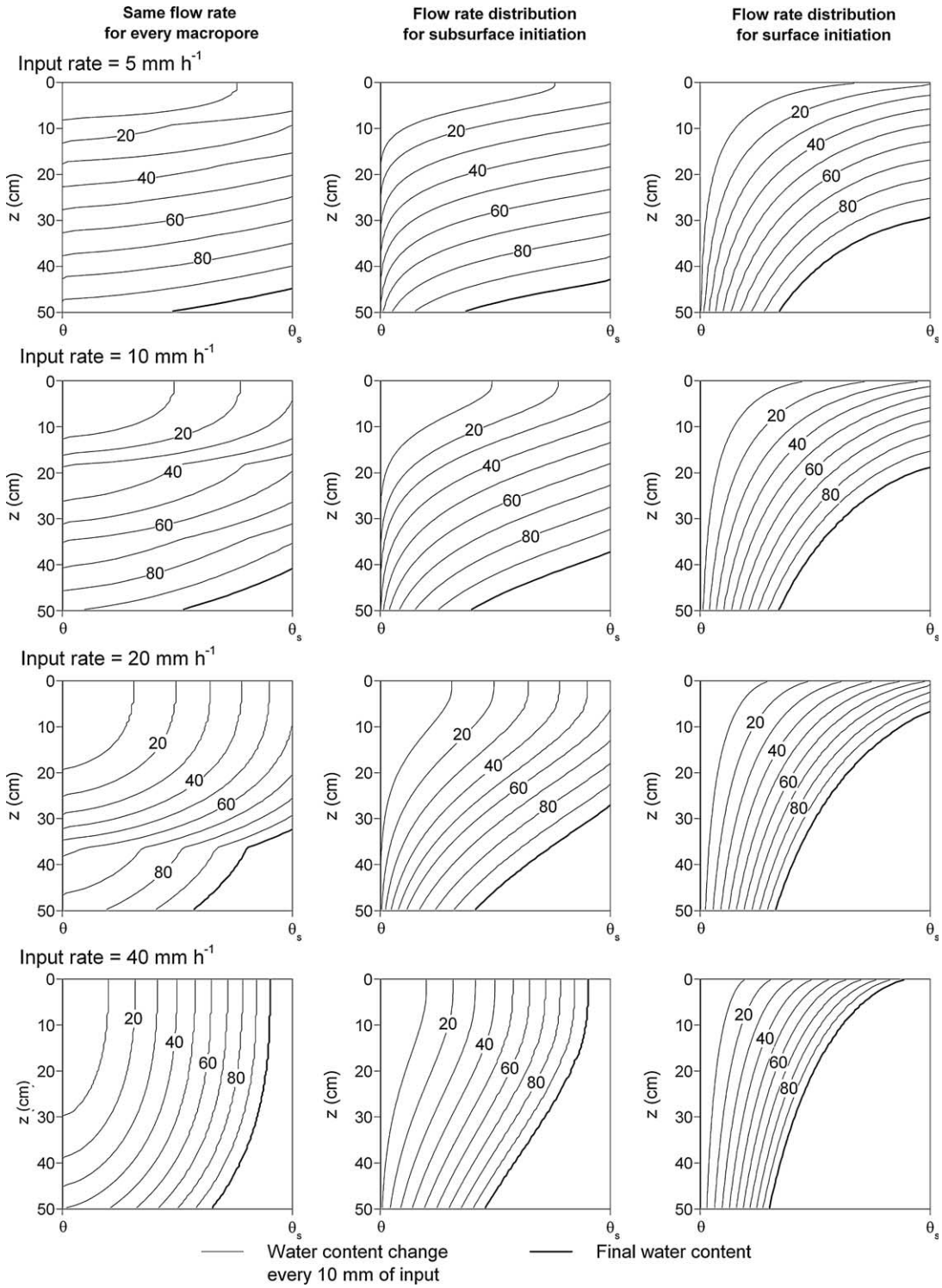

Fig. 3. Simulated temporal water content change in the soil matrix as a function of depth. The isochrones are calculated in flow times referring to the input amount.

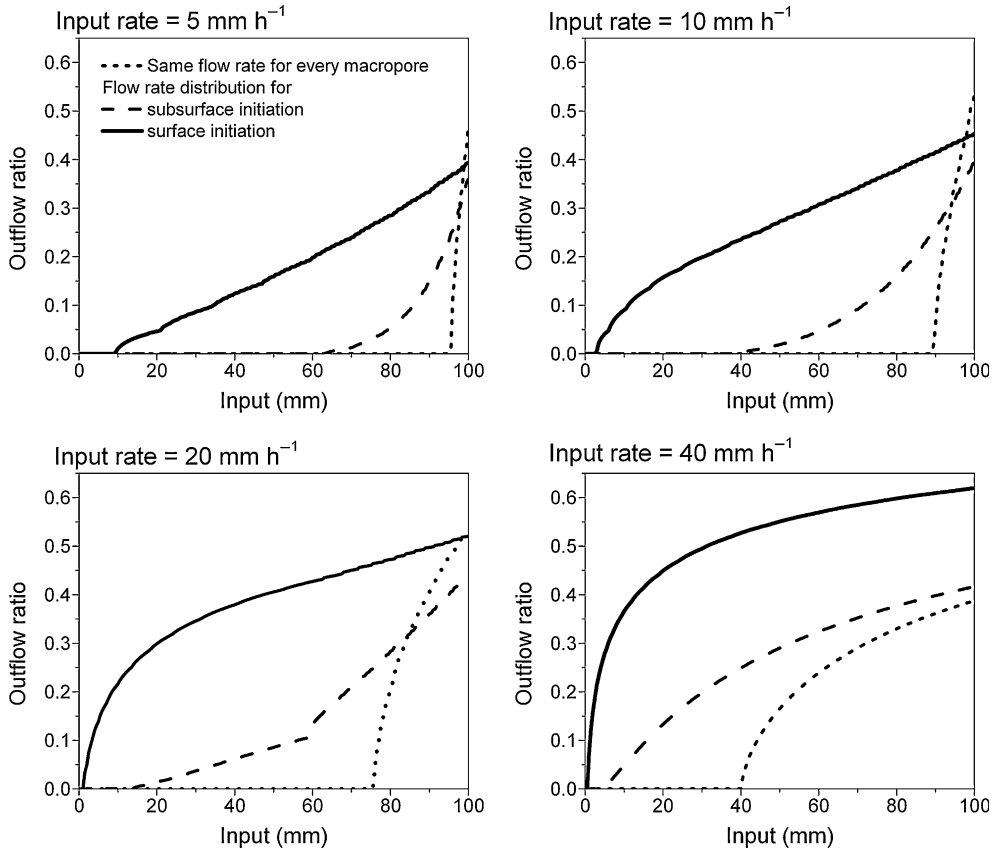

Fig. 4. Simulated outflow rate at the lower boundary for different input rates.

reached the lower boundary. For subsurface initiation, outflow starts after an input of 60 mm, and then increases rapidly. Conversely, the outflow for surface initiation starts after an input of only 10 mm and then increases continuously. This general pattern was also observed for the other input rates. Thus, if the initiation process is considered in modeling infiltration in macroporous soils, outflow starts much faster and can increase rapidly at the beginning.

4. Model application

4.1. Study sites

At three field sites in Northern Switzerland (Heitersberg, Koblenz, and Niederweningen), we conducted sprinkling experiments with a Brilliant Blue solution at two irrigation rates, 60 mm h^{-1} (*high*) and 12 mm h^{-1} (*low*) with a total irrigation of ~75 mm, and two different initial soil moisture conditions referred to as '*dry*' (no input within 4 weeks) and '*wet*' (~75 mm rainfall at the previous day). The dye solution was applied using a sprinkling device consisting of a linearly moving spray bar with 15 flat-spray nozzles moving 1 m above the ground. The sprinkling area was 1 by 1 m. Overland flow from the plot was collected and measured with a tipping bucket (see more details regarding the experimental set-up in Weiler and Naef, 2003a). All of the sites are grassland and their soils exhibit a macropore structure dominated by vertically oriented earthworm burrows (>2 mm diameter). However, other soil characteristics differ (Table 2).

The experimental set-up was optimized to study preferential flow in macroporous soils by combining

Table 2
Soil properties of the experimental sites

Site	Soil classification[a]	Geological parent material	Average values for distinct soil horizon				
			Depth (cm)	Density (g cm^{-3})[b]	Particle size distribution (%)[c]		Soil texture[d]
					Sand	Clay	
Heitersberg	Umbric Cambisol	Moraine	0–20	1.34	36	26	Loam
			20–35	1.57	43	27	Loam
			35–65	1.66	40	23	Loam
			65–100	1.68	57	26	Loam
Koblenz	Eutric Cambisol	Moraine	0–15	1.31	26	23	Silt loam
			15–35	1.35	26	22	Silt loam
			35–60	1.46	26	25	Silt loam
			60–100	1.65	20	30	Silt loam
Niederweningen	Eutric Cambisol	Sandstone (molasse)	0–20	1.41	55	22	Sandy clay loam
			20–40	1.50	60	20	Sandy loam
			40–60	1.44	62	17	Sandy loam
			60–100	1.42	71	11	Sandy loam

[a] Food and Agricultural Organization (1974).
[b] Arithmetic averages of at least 4 samples.
[c] pipette method (sand 2 mm–50 μm, clay <2 μm). % by weight.
[d] Soil Survey Staff (1951).

observations with high spatial and temporal resolution. Data at high temporal but low spatial resolution was derived from detailed soil water content and matric potential measurements (10 TDR probes and 5-6 tensiometer in different depths, see also locations of TDRs in Fig. 5). Data at high spatial but low temporal resolution was derived from dye patterns. The flow pattern of the infiltrated water was visualized by adding 4 g l^{-1} of the food dye Brilliant Blue FCF (C.I. 42090) to the sprinkling water. This dye was chosen because it is a good compromise between visibility, mobility, and toxicity for visualizing flow pathways in the vadose zone (German-Heins and Flury, 2000). Further details about the performed dye pattern analysis can be found in Weiler and Flühler (2004).

4.2. Model parameterization

In a first step of the model application, the input parameters for IN^{3}M were solely derived from different sources described thereafter. The van Genuchten parameters (θ_s, θ_r, α, n) were derived from soil texture, bulk density (see also Table 2) and the water content measurements at 330 kPa using pedotransfer functions (PTFs). These PTFs were based on a large data set to which Schaap et al. (1998) applied a hierarchical approach to estimate hydraulic properties with neural networks. The saturated hydraulic conductivity for the mineral soil layers was estimated from soil texture and bulk density (Schaap and Leij, 2000). Since most PTFs do not incorporate critical soil structural information (Lin et al., 1999a), the predictions for the organic, structure rich A-horizon are quite uncertain for conventional PTFs. Therefore, a 'class PTF' to estimate the hydraulic conductivity for flow in micropores was used to estimate the hydraulic conductivity of the soil matrix for the top layer (Lin et al., 1999b). These class PTFs use textural and morphometric information together with root density and content of organic matter. The macropore properties were determined by image analysis from the classified images of horizontal soil sections (Weiler, 2001). The initial saturation deficit $\Delta\theta$ of each layer was determined from the water content measurements and from the matric potential measurements prior to the experiments. The duration and intensity of the precipitation was directly measured. All input parameters are assembled in Table 3.

The parameter q_{max} describing the maximum outflow of the macropore domain at the lower

Table 3
Input parameters of IN^{3}M for the three experimental sites. The methods to determine the input parameters are explained in the text

Site	Δz (mm)	r (mm)	n_{mac} (m^{-2})	SD_{max}(–)	K_s(mm h^{-1}))	n (–)	α(m^{-1})	$\Delta\theta$(–)
Heitersberg	150	2.4	300	0.33	25.5	1.4	2.1	0.14
	200	3.2	140	0.31	5.0	1.3	1.67	0.10
	300	2.6	140	0.29	1.5	1.3	2.0	0.06
	350	2.6	90	0.29	1.5	1.3	2.0	0.04
	$q_{max}=10.0$ mm h^{-1}							
Koblenz	150	2.0	300	0.36	5.0	1.47	2.1	0.04
	200	2.5	170	0.36	10.0	1.47	1.06	0.02
	250	2.7	200	0.34	4.0	1.52	0.7	0.015
	400	2.8	90	0.30	2.5	1.4	0.9	0.01
	$q_{max}=60.0$ mm h^{-1}							
Niederweningen	200	2.5	250	0.36	4.1	1.38	2.2	0.10
	200	2.7	200	0.34	14.0	1.42	3.0	0.07
	200	2.8	300	0.34	24.0	1.52	3.4	0.07
	200	2.6	200	0.36	55.0	1.84	4.1	0.17
	200	2.6	200	0.34	60.0	1.81	4.3	0.16
	$q_{max}=60.0$ mm h^{-1}							

boundary is the only parameter that cannot be determined directly with this experimental set-up. This parameter could be calibrated to the observations, but we have chosen another strategy by evaluating its sensitivity and together with additional field observation to estimate q_{max}. Therefore, two simulations were carried out to determine the sensitivity of q_{max}. The value of q_{max} was set to zero in the first case and to an unlimited outflow (100 mm h^{-1}) in the second case. The sensitivity of the simulation results to this parameter was determined by comparing the total overland flow (OF) and total water content changes within the soil profile (ΔSM), with the total vertical drainage at the lower boundary (SSF) for the two simulations (Table 4).

For all experiments at the sites of Heitersberg and Koblenz the results show a medium to high influence on diverting the runoff from overland flow to SSF. A low value of q_{max} results in significant overland flow (OF), whereas a high value results in significant

Table 4
Sensitivity of the parameter q_{max} describing the outflow from the macropores at the lower boundary by comparing total overland flow (OF), total water content changes within the soil profile (ΔSM), and total vertical drainage at the lower boundary (SSF)

Site	Experimental conditions		$q_{max}=0$ mm h^{-1}			$q_{max}=100$ mm h^{-1}			Sensitivity of q_{max}
			OF (mm)	ΔSM (mm)	SSF[a] (mm)	OF (mm)	ΔSM (mm)	SSF[b] (mm)	
Heitersberg	High	Dry	33.0	46.7	0.1	1.1	44.3	34.5	High
	High	Wet	59.3	19.9	0.4	1.3	17.5	60.8	High
	Low	Dry	16.6	56.7	0.6	0.0	54.2	19.6	Medium
	Low	Wet	52.9	17.6	6.9	0.0	15.2	62.2	High
Koblenz	High	Dry	25.2	49.6	0.5	1.7	47.0	26.6	Medium
	High	Wet	58.0	18.8	1.5	2.1	16.2	60.0	High
	Low	Dry	14.2	53.4	7.7	0.9	50.8	23.5	Medium
	Low	Wet	40.7	13.2	15.4	1.2	10.7	57.5	High
Niederweningen	High	Dry	3.4	72.0	0.5	3.4	70.3	2.2	Very low
	High	Wet	3.9	71.4	2.1	3.7	67.6	6.1	Low
	Low	Dry	1.7	68.0	1.7	1.7	68.0	1.7	Very low
	Low	Wet	2.5	64.6	11.5	2.5	64.6	11.5	Very low

The overall sensitivity of q_{max} is quantified in the last column.
[a] SSF is only the vertical drainage from the soil matrix.
[b] SSF is the vertical drainage from the soil matrix and the macropore domain.

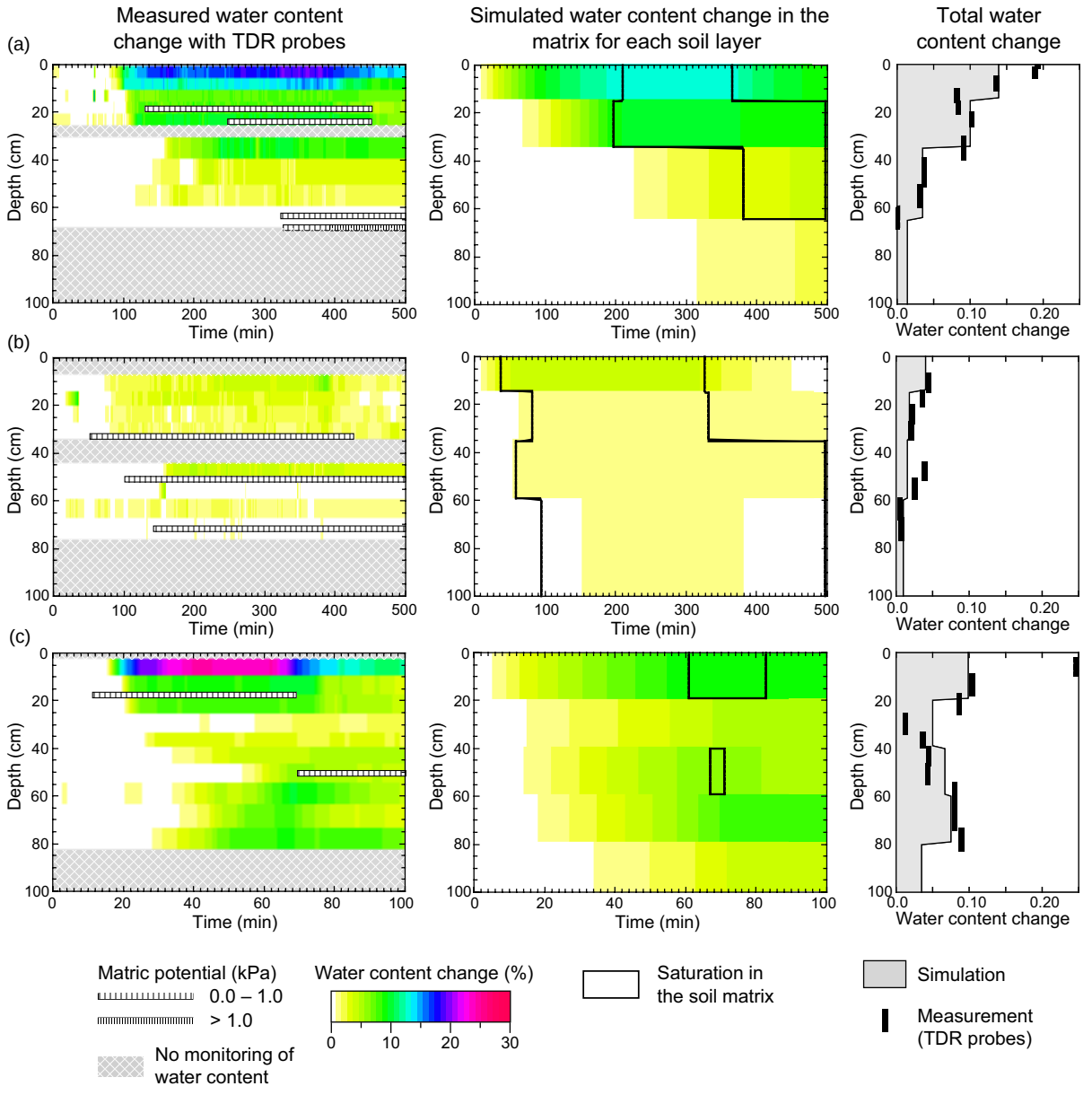

Fig. 5. Water content change criterion for (a) site Heitersberg with low rainfall intensity and dry initial conditions, (b) Koblenz with low rainfall intensity and wet initial conditions, and (c) Niederweningen with high rainfall intensity and wet initial conditions.

subsurface flow (SSF). The soil moisture changes within the soil profile (ΔSM) are similar in both cases, since at the beginning of the experiment the input of water into the macropores and hence the increase of the soil moisture due to interaction is similar. However, later in the experiment for $q_{max}=0$, macropores fill up as soon as the soil is saturated. Since interaction is low, overland flow is initiated. For unlimited outflow, water in the macropores that cannot interact with the soil matrix leaves

the macropores at the lower boundary. Experimental observations at the Heitersberg site for a 1 m^2 plot (Weiler and Naef, 2003a) and for a more representative 60 m^2 hillslope plot (Scherrer, 1997) revealed a significant generation of overland flow for high rainfall intensities (60 mm h^{-1}), but no overland flow generation for low rainfall intensities (12 mm h^{-1}). To reproduce these observations, q_{max} was set to 10 mm h^{-1}. For the Koblenz site, a high value of the maximum outflow and, thus, an unlimited drainage of the macropores results in an agreement with the observed soil moisture changes and overland flow generation. A fast drainage of the macropores could also be experimentally confirmed with observations at a larger scale: dye was observed in the nearby creek 100 m downslope some hours after the beginning of the experiment. Large amounts of dye-colored water had percolated from the macropores into the saturated bedrock and been transported by lateral subsurface flow (Weiler and Naef, 2003a).

The other site, Niederweningen, does not show a marked influence on the parameterization of the macropore outflow since for all experiments the applied water is stored in the soil profile and water did not accumulate in the macropores. Therefore, q_{max} was set equal to the saturated conductivity of the deepest soil layer (Table 3). Finally, it should be noted that q_{max} can be a sensitive parameter in soils with a low saturation deficit and for high rainfall amounts or low potential interaction controlling the switch between runoff generation as overland flow or as subsurface flow.

4.3. Simulation results

The results of the model simulation are described for one selected experiment per site only. They are evaluated separately for the three validation criteria. The water content change criterion shows the measured soil water content change with TDR probes during the sprinkling experiment within a depth–time graph (left column of Fig. 5). The water content value at the beginning of the sprinkling was subtracted from the later observations for each probe segment to obtain the water content changes. In addition, the tensiometer readings are shown by bars indicating the duration and the depth of observed soil saturation. The same information is shown for the simulation (center column of Fig. 5). The right column of Fig. 5 compares the depth distribution of the total water content change. The dye pattern criterion compares the measured and simulated vertical dye patterns and the dye coverage (Fig. 6). The observed vertical dye pattern is one example out of five surveyed dye patterns for each experiment. The simulated dye pattern is a randomly chosen slice from the generated 3D array showing stained and unstained voxels. The observed dye coverage is the average depth function of the dye coverage of the 5 observed vertical dye patterns. The simulated dye coverage is the average depth function from the generated 3D dye pattern. The water balance criterion shows the simulated total water fluxes in the soil matrix, in the macropores, the interaction from the macropores into the surrounding soil matrix and the initiation of macropore flow. The total simulated infiltration, overland flow, and water content change in the soil matrix are compared with measurements (Fig. 7).

The experiment at the Heitersberg site with low rainfall intensity and dry initial soil moisture conditions produced an increase in water content within the topsoil by 10–20% and a small increase ($<5\%$) below 30 cm depth (Fig. 5a). The simulation captures this pattern, especially for the total water content change. Only the timing of water content change in the topsoil and subsoil as well as the saturation of the soil matrix is slightly delayed in the simulation. In accordance with the water content change, the dye pattern shows a pronounced staining of the upper soil layer, whereas the dye coverage below 30 cm depth is low and with small narrow features, indicating a low interaction from the wormholes into the soil matrix (Fig. 6a). The simulation copies the dye staining well, especially the contrast between homogeneous staining in the topsoil and the narrow stained features in the subsoil. A detailed analysis of the experiment showed that macropore flow was initiated from the saturated topsoil layer (Weiler and Naef, 2003a). The simulation reproduced the high proportion of subsurface initiation, as well as the total infiltration and water content change in the soil matrix (Fig. 7a).

As the soil moisture deficit in the soil profile at the Koblenz site was low prior to the experiment with low rainfall intensity, the soil water content change was very low ($<5\%$) and saturation of the soil profile starts within 1–2 h (Fig. 5b). The simulated water

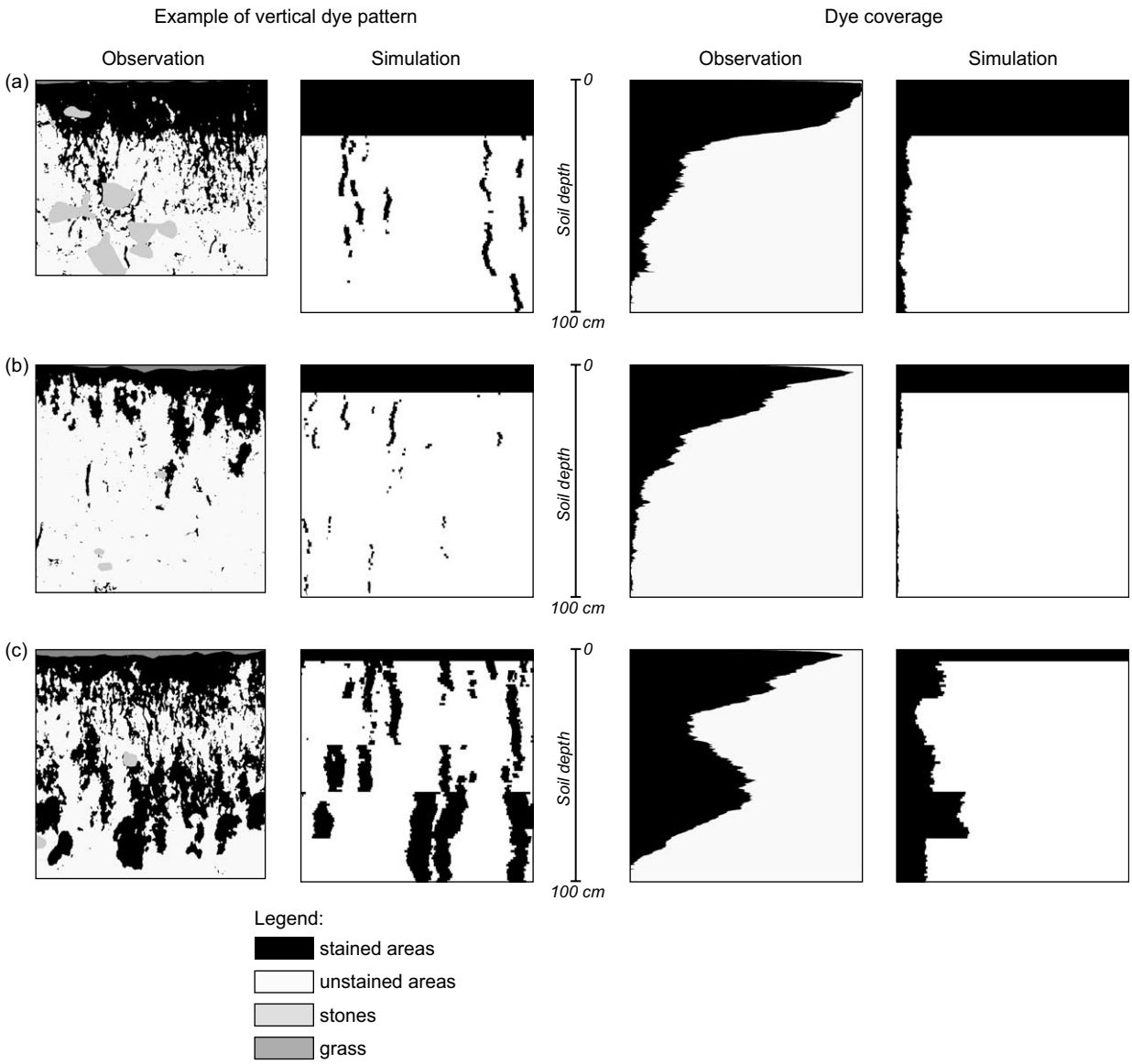

Fig. 6. Dye pattern criterion for (a) site Heitersberg with low rainfall intensity and dry initial conditions, (b) Koblenz with low rainfall intensity and wet initial conditions, and (c) Niederweningen with high rainfall intensity and wet initial conditions.

content change is slightly overestimated and the beginning of saturation starts too early. The dye coverages show an extensively stained upper soil layer, slightly stained subsoil, and a gradual decrease of the dye coverage with depth (Fig. 6b). The dye pattern simulation captures the extensive staining in the topsoil and the narrow stained features in the subsoil, but cannot reproduce the transition between these two regions. The water balance criterion shows that the total infiltration and water content change in the soil matrix is adequately captured, resulting in a high outflow at the lower boundary (Fig. 7b).

The observations for the experiment with high rainfall intensity and wet initial soil moisture conditions at the Niederweningen site show that

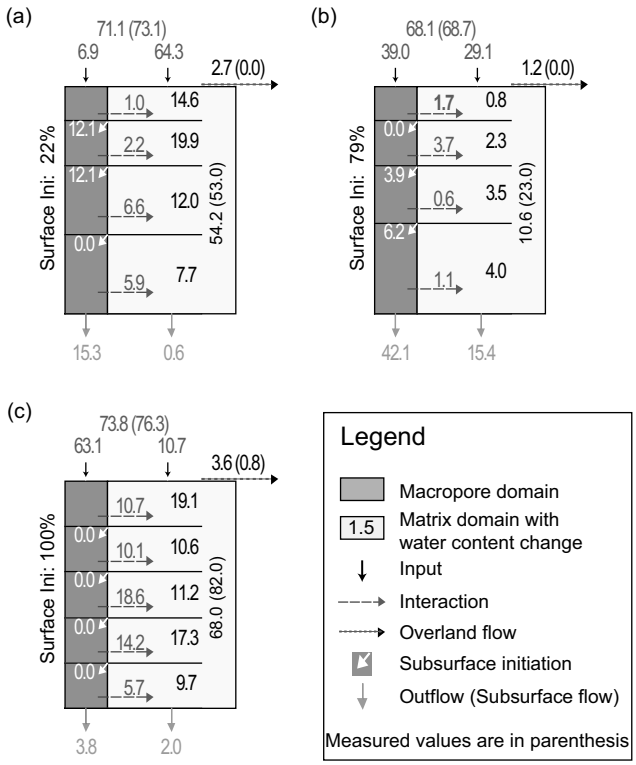

Fig. 7. Water balance criterion (a) site Heitersberg with low rainfall intensity and dry initial conditions, (b) Koblenz with low rainfall intensity and wet initial conditions, and (c) Niederweningen with high rainfall intensity and wet initial conditions.

the water content primarily changed in the top layer (0–30 cm) and in the bottom layer (50–90 cm) (Fig. 5c). The fast tensiometer response in the topsoil was found to be related to a connection of the cup to an earthworm channel and is therefore not representative for the soil matrix saturation. However, this tensiometer reaction immediately after the beginning of the sprinkling can only be explained by an initiation of macropore flow at the soil surface. The water content change simulations agree with the observations (Fig. 5c). Only the final water content change between 20 and 50 cm depth is too high simulated. However, the general pattern of high water content change in the top and bottom layer is well simulated. The observed dye pattern shows a small continuously stained layer at the soil surface that is connected to narrow features indicating low interaction between 20 and 50 cm depth. Below 50 cm, the narrow features expand indicating high water flow from the macropores into the surrounding soil matrix (Fig. 6c). The simulated dye pattern replicates the observed pattern; however, the extreme differences between the narrow and expanded staining are not as pronounced. The dye coverage shows a local minimum at a depth of 30–40 cm; below 40 cm, the staining increases again. The simulated dye coverage reproduces this pattern. However, the depth function of the dye coverage underestimates the observed coverage. The water balance criterion indicates the high interaction of this experiment resulting from the high macropore initiation at the soil surface (Fig. 7c). The simulated total input is in the range of the measured total infiltration. The total water content change in the soil matrix, however, is underestimated. Since the observed water content change is larger than the total infiltration, the TDR measurements probably overestimate the real values.

4.4. Does flow variability matter?

The sensitivity analysis in Section 3 has shown the influence of initiation on interaction for a hypothetical case. Now, the question arises whether the proposed flow variability in the macropores due to the initiation process also matters for the simulations of the three experimental sites? This was examined by simulating the sites with the same flow rate in every macropore instead of considering the probability distribution of surface and subsurface initiation and thus assuming the same flow rate in every macropore. Fig. 8 compares the total interaction at the end of the simulation run with that of the reference simulation. The percentage values give the change of total interaction compared to the reference. For these simulations, the vertical layers thickness was set to 100 mm to show a more detailed depth function of interaction. The results indicate that with the same flow rate in every macropore, interaction for the whole soil profile increases, especially for the high rainfall intensity. The influence is especially pronounced for sites where macropores function to bypass the soil matrix (Heitersberg and Koblenz). The depth distribution of total interaction also changes. Interaction in the upper soil is frequently higher and the percolation depth of macropore flow and, thus, the depth of interaction is significantly lower especially for the Niederweningen site. The influence on the depth distribution of interaction is high for this site, as macropore flow is only initiated at the soil surface (see also Fig. 7) and the soil matrix is very permeable resulting in a high potential interaction. In general, without considering the initiation process, total interaction is overestimated because the same flow rate in every macropore leads to a maximum possible interaction, whereas modeling a flow rate distribution in the macropores results in

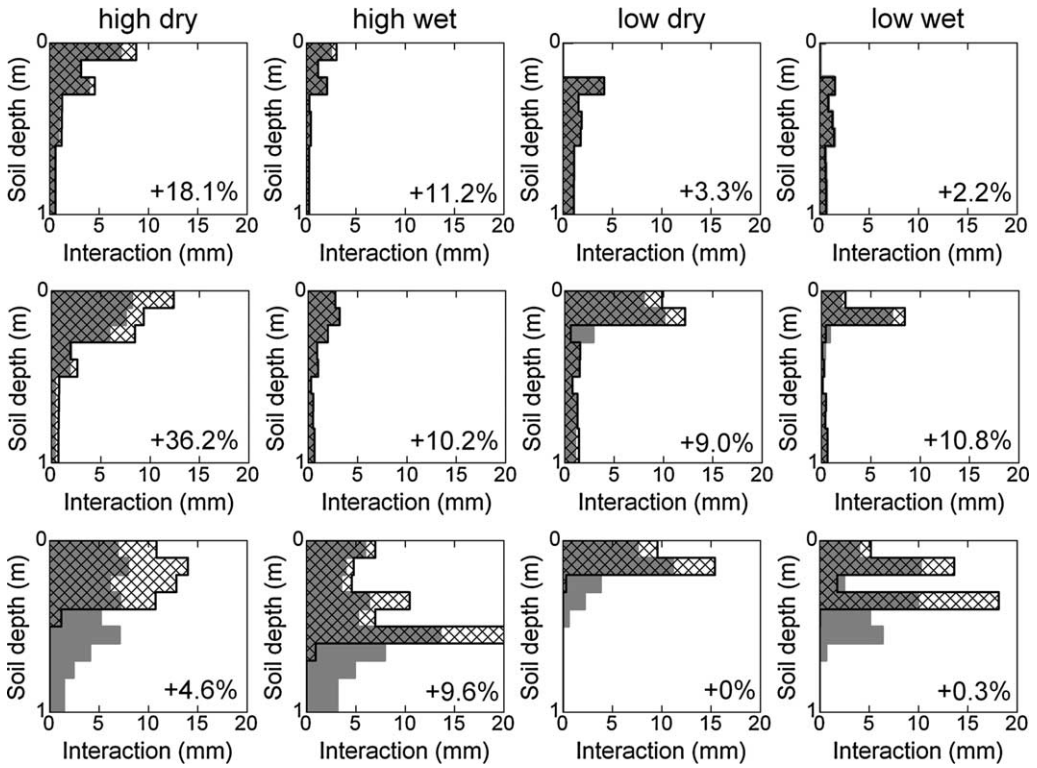

Fig. 8. Total interaction per 10 cm depth interval at the end of the simulation run for the reference simulation (gray area) and the simulation without considering the initiation process (cross hatched area) shown for site (a) Heitersberg, (b) Koblenz, and (c) Niederweningen. The percentage values give the change of total interaction relative to the reference.

a limitation of interaction in part of the macropores. Especially for soils with a high potential interaction, the interaction is higher in the upper soil profile. The effects are more pronounced for surface initiation than for subsurface initiation because the flow rate distribution for surface initiation tends to produce more extreme values. We can conclude from this analysis, that soils that have a limited surface infiltration capacity into the soil matrix, for example as a result of water repellency or soil compaction, in combination with a high interaction capacity, for example in dry soils and/or soil with a high wetting front suction and saturated hydraulic conductivity, will be very sensitive to the consideration of flow variability in the macropores in terms of water content changes and hydrological response of overland flow, subsurface flow and recharge.

5. Discussion

None of the models that describes flow and/or transport in soils containing macropores, like MACRO (Jarvis et al., 1991), QSOIL (Faeh et al., 1997), RZWQM (Ahuja et al., 1995), tipping bucket model (Emerman, 1995), SAMP (Ewen, 1996), LASOMS (Chen and Wagenet, 1992) and PREFLO (Workman and Skaggs, 1990), have yet implemented the variation of flow rate in macropores due to the initiation process. This study assessed the hypothesis that the flow rate distribution in macropores due to the initiation process is crucial to infiltration in macroporous soils and hence to runoff generation in general. The results for the hypothetical case and for the application to the three field sites revealed that interaction is regularly overestimated and thus preferential flow is underestimated. The degree of influence, however, strongly depends on the rainfall rate and the type of initiation process. For extreme precipitation events, which occur with a low probability, but may cause floods and/or large export of nutrients, solutes, and sediments, this study demonstrated that it is important to consider the macropore flow rate distribution when simulating infiltration in macroporous soils. The higher influence under higher rainfall intensity is related to the higher probability of initiating macropore flow at the soil surface, since surface initiation causes a flow rate distribution with a high skewness, meaning only a few macropores contribute significantly to the water flow (Weiler and Naef, 2003b). Since neither the surface roughness, the slope, nor the macropore density influence the shape of the distribution significantly, we can assume that only the probability of occurrence of surface initiation and the macropore density affects the individual inflow into each macropore (see also Eq. (1)). However, even for cases with dominating subsurface initiation (e.g. Heitersberg and Koblenz for 'low' rainfall intensities), interaction is overestimated and the hydrological response is underestimated. Thus, if the initiation process is considered in modeling infiltration in macroporous soils, the hydrological response of a site in terms of overland flow, subsurface flow, or recharge to the groundwater starts earlier and responses more rapidly.

Researchers have attributed the overestimation of interaction that was simulated frequently with dual-permeability models to the deposition of organic matter, various types of coatings, fine texture material particles, or various oxides and hydroxides on the macropore walls (Larsson and Jarvis, 1999; Saxena et al., 1994). These coatings can markedly reduce rates of water transfer between macropores and the soil matrix (Thoma et al., 1992; Gerke and Köhne, 2002). However, as the presented study shows, the flow rate distribution in the macropores can also explain observed reductions in interaction. It may be a combination of the flow rate distribution, the coating of the macropore wall, and the incomplete wetting of the macropore-matrix interface act collectively to reduce the total interaction between macropores and soil matrix and thus enhance bypassing. The importance of the individual explanations may result from the soil properties, the type and density of macropores, and the rainfall intensity characterizing a site. Nevertheless, laboratory studies using grid lysimeters showed a high variability of water and solute flux on the lower boundary, which would support the assumption of a flow rate distribution in macropores. For example, Edwards et al. (1992) measured percolate for a soil block with macropores formed by *Lumbricus terrestris* and found one grid cell comprised 30–60% of total percolate. Since we may be able to measure the hydraulic properties of the macropore wall (Gerke and Köhne, 2002) or to directly measure the water transfer between

macropores and the soil matrix in the field using devices like a macropore infiltrometer (Wang et al., 1994), future research may shed more light on the importance of the individual processes.

Despite the quite rudimentary parameter estimation methods for the soil hydraulic properties using two types of PTFs and for the visible macropore system using image analysis of horizontal soil sections, the simulation results of IN^{3}M were surprisingly satisfying when evaluated with the multi-criteria validation strategy. However, it is necessary to mention that the parameter q_{max} accounting for the lower boundary condition of the macropore domain could not be determined a priori with this experimental set-up, since quantitative information regarding the connection of vertical macropores with lateral preferential flow pathways was missing. The simulation results revealed that this parameter has a significant effect for certain soils on the simulation results diverting the runoff either to overland flow or to vertical drainage at the lower boundary of the soil profile. The relativly high rainfall intensities (60 and 12 mm h^{-1}) chosen for the field experiments and thus for the simulations also favor the introduced model, since it is strongly oriented toward infiltration during flood generating rainfall events. However, the focus of this study is flow variability in macropores, and how this influences interaction and infiltration. Given this, the introduced model provides only a suggestion regarding the incorporation of macropore flow variability into well-known concepts used in other dual permeability models.

Finally, we believe that new directions in model verification and calibration are necessary to overcome the fact that our measurements do not often correspond to the spatial and/or temporal scales of our models. For example, the point measurements of water content using TDRs or matric potential using tensiometers will, especially under preferential infiltration behavior, probably not be reliable methods to determine the average water content change for a soil layer. And even outflow measurements from smaller scale lysimeters (<0.5 m^2) may not reflect the real average percolation flux due to a high spatial variability of preferential flow. Therefore, we strongly urge to apply a multi-criteria validation strategies combining data of high spatial, but low temporal information content (e.g. dye pattern) with data of low spatial but high temporal information content (e.g. TDR and tensiometer measurements). In this study, we only used a qualitative comparison of the agreement of the simulated with the observed criteria since, for example, a quantitative criterion to compare the structure of dye patterns is not yet developed. However, we believe that a variety of possibilities exists to develop quantitative measures using more complex data structures in the future. (e.g. Flühler and Weiler, 2004).

6. Conclusion

Evaluating and testing a model (IN^{3}M) that combines well-known approaches of simulating initiation and interaction with the yet uncommon initiation-based flow rate distribution demonstrated that the initiation process is crucial to correctly simulate infiltration in macroporous soils. Without considering the initiation process, total water flux from the macropores into the soil matrix is overestimated and thus hydrological response is underestimated. Further work is necessary to explore the flow variability in macropores and its effect on model predictions of water and solute transport for soils that contain different types of macropores and for other initial and boundary conditions. However, this study shows that including macropore flow variability into a dual permeability model framework promises significant progress in our ability to model and predict macropore flow.

Acknowledgements

This work was funded by the Swiss Federal Institute of Technology in Zürich within the project ‘Investigation of the water exchange mechanisms between preferential flow paths and the soil matrix’. I would like to thank Felix Naef for his support during this study and especially Thomy Keller for his help during the field experiments. Kerstin Stahl, Kevin McGuire, and Kellie Vache provided helpful comments on the manuscript.

References

Ahuja, L.R., Johnsen, K.E., Heathman, G.C., 1995. Macropore transport of a surface applied bromide tracer: model evaluation and refinement. Soil Sci. Soc. Am. J. 59, 1234–1241.

Ahuja, L.R., Rojas, K.W., Hanson, J.D., Shaffer, M.J., Ma, L. (Eds.), 2000. Root Zone Water Quality Model-Modelling Management Effects on Water Quality and Crop Production. Water Resources Publications, Highlands Ranch, Colorado, p. 372.

Beckers, J., Alila, Y., 2004. A model of rapid preferential hillslope runoff contributions to peakflow generation in a temperate rainforest watershed. Water Resour. Res. 40, w03501. DOI:10.1029/2003WR002582.

Beven, K.J., 2001. Rainfall-Runoff Modelling: The Primer. John Wiley, Chichester, England pp. 360.

Beven, K., Germann, P., 1982. Macropores and water flow in soils. Water Resour. Res. 18 (5), 1311–1325.

Beven, K.J., Clarke, R.T., 1986. On the variation of infiltration into a homogeneous soil matrix containing a population of macropores. Water Resour. Res. 22 (3), 383–388.

Bouma, J., Belmans, C.F.M., Dekker, L.W., 1982. Water infiltration and redistribution in a silt loam subsoil with vertical worm channels. Soil Sci. Soc. Am. J. 46, 917–921.

Bronstert, A., 1999. Capabilities and limitations of detailed hillslope hydrological modelling. Hydrologic. Process 13, 121–148.

Burch, G.J., Moore, I.D., Burns, J., 1989. Soil hydrophobic effects on infiltration and catchment runoff. Hydrologic. Process 3, 211–222.

Buttle, J.M., Leigh, D.G., 1997. The influence of artificial macropores on water and solute transport in laboratory soil columns. J. Hydrol. 191, 290–313.

Chen, C., Wagenet, R.J., 1992. Simulation of water and chemicals in macropore soils. Part 1. Representation of the equivalent macropore influence and its effect on soilwater flow. J. Hydrol. 130, 105–126.

Edwards, W.M., Shipitalo, M.J., Dick, W.A., Owens, L.B., 1992. Rainfall intensity affects transport of water and chemicals through macropores in no-till soil. Soil Sci. Soc. Am. J. 56, 52–58.

Ela, S.D., Gupta, S.C., Rawls, W.J., 1992. Macropore and surface seal interactions affecting water infiltration into soils. Soil Sci. Soc. Am. J. 56, 714–721.

Emerman, S.H., 1995. The tipping bucket equations as a model for macropore flow. J. Hydrol. 171, 23–47.

Ewen, J., 1996. SAMP model for water and solute movement in unsaturated porous media involving thermodynamic subsystems and moving packets: 1. Theory. J. Hydrol. 182, 175–194.

Faeh, A.O., Scherrer, S., Naef, F., 1997. A combined field and numerical approach to investigate flow processes in natural macroporous soils under extreme precipitation. Hydrol. Earth Syst. Sci. 1 (4), 787–800.

Flury, M., Wai, N.N., 2003. Dyes as tracers for vadose zone hydrology. Rev. Geophysics 41 (1). 10.1029/2001RG000109.

Gerke, H.H., Köhne, J.M., 2002. Estimating hydraulic properties of soil aggregate skins from sorptivity and water retention. Soil Sci. Soc. Am. J. 66, 26–36.

German-Heins, J., Flury, M., 2000. Sorption of brilliant blue FCF in soils affected by pH and ionic strength. Geoderma 97, 87–101.

Germann, P., Beven, K., 1981. Water flow in soil macropores III. A statistical approach. J. Soil Sci. 32, 31–39.

Ghodrati, M., Chendorain, M., Chang, Y.J., 1999. Characterization of macropore flow mechanisms in soil by means of a split macropore column. Soil Sci. Soc. Am. J. 63, 1093–1101.

Green, W.H., Ampt, G.A., 1911. Studies of soil physics. I. The flow of air and water through soils. J. Agric. Sci. 4, 1–24.

Jarvis, N.J., Jansson, P.E., Dik, P.E., Messing, I., 1991. Modeling water and solute transport in macroporous soil. I. Model description and sensitivity analysis. J. Soil Sci. 42, 59–70.

Kiang, T., 1966. Random fragmentation in two and three dimensions. Zeitschrift für Astrophysik 64, 433–439.

Klemes, V., 1986. Dilettantism in hydrology: transition or destiny?. Water Resour. Res. 22 (9), 177S–188S.

Langmaack, M., Schrader, S., Rapp-Bernhardt, U., Kotzke, K., 1999. Quantitative analysis of earthworm burrow systems with respect to biological soil–structure regeneration after soil compaction. Biol. Fertil. Soils 28, 219–229.

Larsson, M.H., 1999. Quantifying macropore flow effects on nitrate and pesticide leaching in a structured clay soil, Field Experiments and Modelling with the MACRO and SOILN Models 1999.

Larsson, M.H., Jarvis, N.J., 1999. Evaluation of a dual-porosity model to predict field-scale solute transport in a macroporous soil. J. Hydrol. 215, 153–171.

Legates, D.R., McCabe, G.J., 1999. Evaluating the use of goodness-of-fit measures in hydrologic and hydroclimatic model validation. Water Resour. Res. 35 (1), 233–241.

Léonard, J., Esteves, M., Perrier, E., de Marsily, G., 1999. A spatialized overland flow approach for the modelling of large macropores influence on water infiltration, International Workshop of EurAgEng's Field of Interest on Soil and Water, Leuven, pp. 313–322.

Léonard, J., Perrier, E., de Marsily, G., 2001. A model for simulating the influence of a spatial distribution of large circular macropores on surface runoff. Water Resour. Res. 37 (12), 3217–3225.

Li, Y., Ghodrati, M., 1997. Preferential transport of solute through soil columns containing constructed macropores. Soil Sci. Soc. Am. J. 61, 1308–1317.

Ligthart, T.N., Peek, G.J.C.W., 1997. Evolution of earthworm burrow systems after inoculation of lumbricid earthworms in a pasture in the Netherlands. Soil Biol. Biochem. 29 (3/4), 453–462.

Lin, H.S., McInnes, K.J., Wilding, L.P., Hallmark, C.T., 1999a. Effects of soil morphology on hydraulic properties I. Quantification of soil morphology. Soil Sci. Soc. Am. J. 63, 948–954.

Lin, H.S., McInnes, K.J., Wilding, L.P., Hallmark, C.T., 1999b. Effects of soil morphology on hydraulic properties II. Hydraulic pedotransfer functions. Soil Sci. Soc. Am. J. 63, 955–961.

LogsdonM, S.D., Nachabe, M.H., Ahuja, L.R., 1996. Macropore Modeling: State of the Science. Water Resources Research Institute, Colorado State University, Fort Collins. Information Series No. 86.

McDonnell, J.J., 1990. A rationale for old water discharge through macropores in a steep, humid catchment. Water Resour. Res. 26 (11), 2821–2832.

Mein, R.G., Larson, C.L., 1973. Modelling infiltratiuon during a steady rain. Water Resour. Res. 9 (2), 384–394.

Návar, J., Turton, D.J., Miller, E.L., 1995. Estimating Macropore and Matrix Flow Using the Hydrograph Separation Procedure in an Experimental Forest Plot 1995.

Niehoff, D., Fritsch, U., Bronstert, A., 2002. Land-use impacts on storm-runoff generation: scenarios of land-use change and simulation of hydrological response in a meso-scale catchment in SW-Germany. J. Hydrol. 267 (1), 80–94.

Perret, J., Prasher, S.O., Kantzas, A., Langford, C., 1999. Three-dimensional quantification of macropore networks in undisturbed soil cores. Soil Sci. Soc. Am. J. 63, 1530–1543.

Saxena, R.K., Jarvis, N.J., Bergström, L., 1994. Interpreting non-steady state tracer breakthrough experiments in sand and clay soils using a dual-porosity model. J. Hydrol. 162, 279–298.

Schaap, M.G., Leij, F.J., 2000. Improved prediction of unsaturated hydraulic conductivity with the Mualem-van Genuchten model. Soil Sci. Soc. Am. J. 64, 843–851.

Schaap, M.G., Leij, F.J., van Genuchten, M.T., 1998. Neural network analysis for hierarchical prediction of soil hydraulic properties. Soil Sci. Soc. Am. J. 62, 847–855.

Scherrer, S., 1997. Abflussbildung bei Starkniederschlägen, Identifikation von Abflussprozessen mittels künstlicher Niederschläge 1997.

Schiffler, G.R., 1992. Experimentelle Erfassung und Modellierung der Infiltration stärkerer Niederschläge unter realen Feldbedingungen 1992.

Seibert, J., McDonnell, J.J., 2002. On the dialog between experimentalist and modeler in catchment hydrology: use of soft data for multicriteria model calibration. Water Resour. Res. 38. 10.1029/2001WR000978.

Shipitalo, M.J., Gibbs, F., 2000. Potential of earthworm burrows to transmit injected animal wastes to tile drain. Soil Sci. Soc. Am. J. 64, 2103–2109.

Simunek, J., Jarvis, N.J., van Genuchten, M.T., Gardenas, A., 2003. Review and comparison of models for describing non-equilibrium and preferential flow and transport in the vadose zone. J. Hydrol. 272 (1), 14–35.

Smettem, K.R.J., 1986. Analysis of water flow from cylindrical macropores. Soil Sci. Soc. Am. J. 50, 1139–1142.

Smettem, K.R.J., Chittleborough, D.J., Richards, B.G., Leaney, F.W., 1991. The influence of macropores on runoff generation from a hillslope soil with a contrasting textural class. J. Hydrol. 122, 235–252.

Syers, J.K., Springett, J.A., 1983. Earthworm ecology in grassland soils, in: Satchell, J.E. (Ed.), Earthworm Ecology. Chapman and Hall, , pp. 67–83.

Thoma, S.G., Gallegos, D.P., Smith, D.M., 1992. Impact of fracture coatings on fracture/matrix flow interactions in unsaturated, porous media. Water Resour. Res. 28, 1357–1367.

Trojan, M.D., Linden, D.R., 1992. Microrelief and rainfall effects on water and solute movement in earthworm burrows. Soil Sci. Soc. Am. J. 56, 727–733.

van Genuchten, M.T., 1980. A closed-form equation for predicting the hydraulic conductivity of unsaturated soils. Soil Sci. Soc. Am. J. 44, 892–898.

van Stiphout, T.P.J., van Lanen, H.A.J., Boersma, O.H., Bouma, J., 1987. The effect of bypass flow and internal catchment of rain on the water regime in a clay loam grassland soil. J. Hydrol. 95, 1–11.

Wang, D., Norman, J.M., Lowery, B., McSweeney, K., 1994. Nondestructive determination of hydrogeometrical characteristics of soil macropores. Soil Sci. Soc. Am. J. 58 (2), 294–303.

Weiler, M., 2001. Mechanisms controlling macropore flow during infiltration-dye tracer experiments and simulations, ETHZ, Zürich, Switzerland, 151 pp.

Weiler, M., Flühler, H., 2004. Inferring flow types from dye patterns in macroporous soils. Geoderma 120 (1–2), 137–153.

Weiler, M., McDonnell, J., 2004. Virtual experiments: a new approach for improving process conceptualization in hillslope hydrology. J. Hydrol. 285 (1–4), 3–18.

Weiler, M., Naef, F., 2003a. An experimental tracer study of the role of macropores in infiltration in grassland soils. Hydrologic. Process 17 (2), 477–493.

Weiler, M., Naef, F., 2003b. Simulating surface and subsurface initiation of macropore flow. J. Hydrol. 273, 139–154.

Weiler, M., Naef, F., Leibundgut, C., 1998. Study of runoff generation on hillslopes using tracer experiments and physically based numerical model. IAHS Publication 248, 353–360.

Workman, S.R., Skaggs, R.W., 1990. PREFLO: A water management model capable of simulating preferential flow. Trans. ASAE 33 (6), 1938–1939.